Hierarchy of anomalies in the two-dimensional Mercedes-Benz model of water

Tomaz Urbic*
University of Ljubljana, Faculty of Chemistry and Chemical Technology, Večna pot 113, SI-1000 Ljubljana, Slovenia

Ken A. Dill
Laufer Center for Physical and Quantitative Biology, Stony Brook University, Stony Brook, New York 11794-5252, USA

(Received 14 September 2017; revised manuscript received 24 August 2018; published 11 September 2018)

We investigate by Monte Carlo simulations density, diffusion, and structural anomalies of the simple two-dimensional Mercedes-Benz (MB) model of water, which is a very simple toy model for explaining the origin of water properties. MB water molecules are modeled as two-dimensional Lennard-Jones disks, with three orientation-dependent hydrogen-bonding arms, arranged as in the MB logo. The model is in a way also a variance of silica-like models. Beside the known thermodynamic anomaly for the model we also found diffusion and structural anomalies and map out the cascade of density, structural, pair entropy, and diffusivity anomalies for MB model. The orientational order parameters with three and six-fold symmetry were determined and maximum for each one observed. The anomalies occur in hierarchy order, which is a slight variation of the hierarchy order in real water. The diffusion anomaly region is the innermost in the hierarchy while for water it is the density anomaly region.

DOI: 10.1103/PhysRevE.98.032116

I. INTRODUCTION

Anomalous liquids are liquids that exhibit unexpected behavior upon variations of the thermodynamic conditions in comparison to normal (argon-like) liquids. Water is the classic example of those anomalous liquids. There are two very distinct mechanisms that give rise to the anomalous properties. Angular-dependent interactions, such as oriented hydrogen bonding in water, tetrahedral bonding in silica [1–3], and oriented bonds in BeF_2, can result in density maximum because of the competition between tetrahedral order (low density) and translational order (high density). On the other hand, density anomaly was also observed for Ga [4], Bi [5], Te [6], S [7], Be, Mg, Ca, Sr, Ba, P, Se, Ce, Cs, Rb, Co, Ge where the system lacked oriented bonding. Speaking of water, it expands upon cooling at fixed pressure, diffuses faster upon compression at fixed temperature [8,9], and becomes less ordered upon increasing density at constant temperature [10]. These are the density, diffusion, and structural anomalies. The regions in which these anomalies occur form nested domes in the density-temperature diagram [10] or pressure-temperature diagram [11]. The structural anomaly domain occupies the outer region of the pressure temperature phase diagram and the density anomaly region is the innermost region for water-like fluids. The diffusion anomaly region lies between these two domains [10,11]. This is called the hierarchy of water anomalies. It must be noted, however, that for different compounds not all anomalies always appear and that a detailed understanding of their origin and their hierarchy remain elusive [12,13].

A large number of models of varying complexity have been developed and analyzed to model water's extraordinary properties, for reviews, see, e.g., [14–17]. Many properties of water and aqueous solutions can be captured by simpler models [18,19]. One class of such simpler models has been developed by Nezbeda and coworkers [15,20,21]. There are also many other simple models [22–26]. One the simplest models for water is the so-called Mercedes-Benz (MB) model [27–31], which was originally proposed by Ben-Naim in 1971 [32,33]. This is a two-dimensional toy model where each water molecule is modeled as a disk that interacts with other such waters through: (1) a Lennard-Jones (LJ) interaction and (2) an orientation-dependent hydrogen bonding interaction through three radial arms arranged as in the Mercedes-Benz (MB) logo. Interest in simplified models is due to insights that are not obtainable from all-atom computer simulations. Simpler models are more flexible in providing insights and illuminating concepts, and they do not require big computer resources. Second, the simple models can explore a much broader range of conditions and external variables. Whereas simulating a detailed model may predict the behavior at one temperature and pressure, a simpler model can be used to study a whole phase diagram of temperatures and pressures. Third, the analytical models can provide functional relationships for engineering applications and lead to improved models of greater computational efficiency. Fourth, simple models can be used as a polygon to develop and study theoretical methods. Our interest in using the MB is that it serves as one of the simplest models of an orientationally dependent liquid, so it can serve as a testbed for developing analytical theories that might ultimately be useful for more realistic models. Another advantage of the MB model, compared to the more realistic water models, is that the underlying physical principles can be more readily explored and visualized in two

*tomaz.urbic@fkkt.uni-lj.si

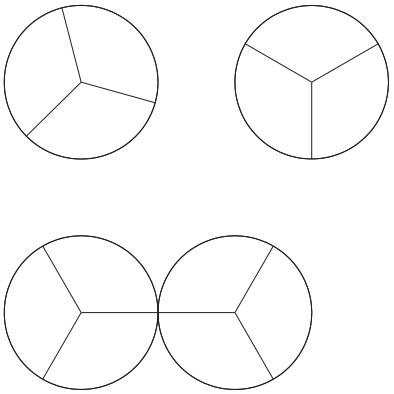

FIG. 1. The MB molecules. Particles form the strongest hydrogen bond when the arms are colinear and the distance between the two particles is equal to r_{HB}.

dimensions. For the MB model, the NPT Monte Carlo simulations have shown that the MB model predicts qualitatively the density anomaly, the minimum in the isothermal compressibility as a function of temperature, the large heat capacity, as well as the experimental trends for the thermodynamic properties of the solvation of nonpolar solutes [28,30,31,34] and cold denaturation of proteins [35]. The two-dimensional (2D) MB model was also extended to three dimensions by Bizjak *et al.* [36,37] and Dias *et al.* [34,38] and studied using computer simulations [34,36–38]. The 2D model was also extensively studied with analytical methods like integral equation and thermodynamic perturbation theory [39–45].

In this paper, we investigate the presence of the anomalies in a simple 2D MB model of water in Fig. 1. We determine the density, diffusion, and structural anomalies and we observe that they occur with a hierarchy slightly different as in water. The outline of the paper is as follows. We present the MB model in Sec. II, and the details of the Monte Carlo simulations in Sec. III. In Sec. IV we show and discuss the results and summarize everything in Sec. V.

II. MODEL

In the framework of the MB model of water the water molecules are modelled as a 2D disk with three bonding arms separated by an angle of 120° [28,32] which is fixed. These arms mimic the formation of hydrogen bonds. The interaction potential between water particles i and j is a sum of a Lennard-Jones (LJ) and a hydrogen-bonding (HB) term

$$U(\vec{X}_i, \vec{X}_j) = U_{\mathrm{LJ}}(r_{ij}) + U_{HB}(\vec{X}_i, \vec{X}_j), \tag{1}$$

where r_{ij} is the distance between the centers of particles i and j. $\vec{X}_i$ and $\vec{X}_j$ are the vectors representing the coordinates and the orientation of the ith and jth molecule. The Lennard-Jones part of the potential has a standard form

$$U_{\mathrm{LJ}}(r_{ij}) = 4\varepsilon_{\mathrm{LJ}}\left[\left(\frac{\sigma_{LJ}}{r_{ij}}\right)^{12} - \left(\frac{\sigma_{LJ}}{r_{ij}}\right)^{6}\right], \tag{2}$$

where $\varepsilon_{\mathrm{LJ}}$ is the depth and σ_{LJ} the contact value. The hydrogen bonding part of the potential is the sum of interactions U^{kl}_{HB}

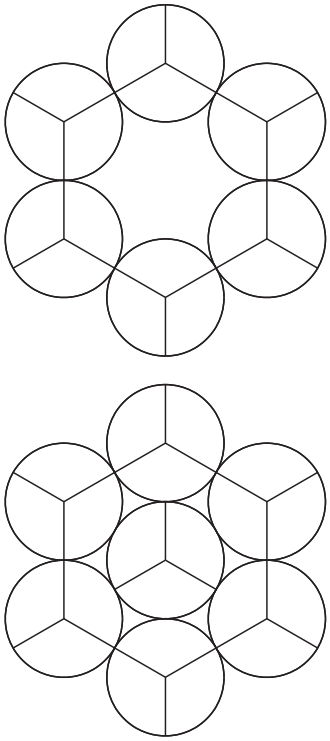

FIG. 2. (a) The unit cell of the low density ice. (b) The unit cell of the high density ice.

between all arms of different molecules

$$U_{\mathrm{HB}}(\vec{X}_i, \vec{X}_j) = \sum_{k,l=1}^{3} U^{kl}_{\mathrm{HB}}(r_{ij}, \theta_1, \theta_2). \tag{3}$$

This interaction is described by the Gaussian function in distance and both angles

$$U^{kl}_{\mathrm{HB}}(r_{ij}, \theta_1, \theta_2) = \varepsilon_{\mathrm{HB}} G(r_{ij} - r_{\mathrm{HB}}) G(\vec{i}_k \vec{u}_{ij} - 1) G(\vec{j}_l \vec{u}_{ij} + 1) \tag{4}$$

$$= \varepsilon_{\mathrm{HB}} G(r_{ij} - r_{\mathrm{HB}}) \times G\left\{\cos\left[\theta_i + \frac{2\pi}{3}(k-1)\right] - 1\right\} \times G\left\{\cos\left[\theta_j + \frac{2\pi}{3}(l-1)\right] + 1\right\}. \tag{5}$$

Here $\varepsilon_{\mathrm{HB}} = -1$ is a HB energy parameter and $r_{\mathrm{HB}} = 1$ is a characteristic length of hydrogen bond. $\vec{u}_{ij}$ is the unit vector along $\vec{r}_{ij}$ and $\vec{i}_k$ is the unit vector representing the kth arm of the ith particle. θ_i is the orientation of the ith particle with respect to the x axes. $G(x)$ is an unnormalized Gaussian function

$$G(x) = \exp\left(-\frac{x^2}{2\sigma^2}\right). \tag{6}$$

The strongest hydrogen bond occurs when an arm of one particle is colinear with the arm of another particle and the two arms point in opposing directions. The LJ well-depth $\varepsilon_{\mathrm{LJ}}$ is 0.1 times the HB interaction energy $\varepsilon_{\mathrm{HB}}$ and the Lennard-Jones contact parameter σ_{LJ} is $0.7r_{\mathrm{HB}}$. The width of the Gaussian for

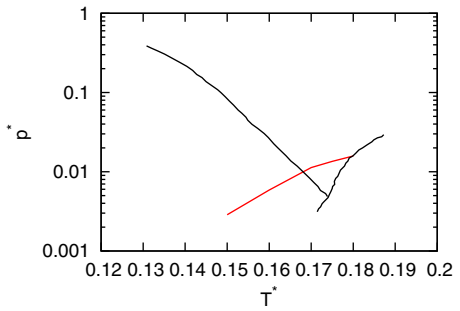

FIG. 3. $T^* - p^*$ phase diagram from MC simulations. Red curve are results for gas-liquid coexistence by Urbic [45] in comparison to the prediction of the phase diagram by Silverstain *et al.* [29], which is plotted by the black line.

distances and angles ($\sigma = 0.085 r_{\mathrm{HB}}$) is small enough that a direct hydrogen bond is more favorable than a bifurcated one.

III. MONTE CARLO COMPUTER SIMULATION

To determine anomalies and their hiererchy in the 2D MB model of water we performed Monte Carlo computer simulations in canonical ensemble (constant N, V, and T) [46,47]. To mimic an infinite size of system of particles we used the periodic boundary conditions and the minimum image convention. All starting configurations were selected at random. Each move consisted of a translation of a random particle and rotation of a different random particle. The probabilities for translation and rotation were the same. In one cycle (also one time step) we tried to translate and rotate each particle once on average. The simulations were equilibrated for 5 000 000 cycles and averages were taken for 20 series each consisted for another 5 000 000 cycles to obtain well-converged results. In the system we had from 100 to 500 particles depending on the density of the system. We used such a number of particles that the increase of this number had no significant effect on the calculated quantities. The system of 100 molecules in two dimensions is equivalent to 1000 particles in three dimensions although 2D systems are more complicated in comparison to the three-dimensional (3D) ones. It is well known that when confined to a 2D space, condensed matter behaves differently than in three dimensions. An example is provided by 2D crystals, where thermal fluctuations are so strong as to rule out long-range translational order for nonzero temperatures, leaving it open for the possibility of unconventional melting scenarios [48]. Thermodynamic quantities such as energy were calculated as statistical averages over the course of the simulations [47]. The cutoff of the potential was the half-length of the simulation box. The pressure was calculated by means of a virial equation [47].

The diffusion coefficient is determined using the mean square displacement averaged over different series. In these MC simulation runs, the dynamic adjustment of maximum displacement was turned off and was kept fixed for all instances. The mean square displacement was calculated as the average of displacements over all particles

$$\langle \Delta r(n)^2 \rangle = \langle [\vec{r}(n) - \vec{r}_0]^2 \rangle, \tag{7}$$

where $\vec{r}_0$ is the initial coordinate of the particle and n is the number of cycles. The pseudodiffusion coefficient which is proportional to the real diffusion coefficient was obtained as

$$D^* = \lim_{n\to\infty} \frac{\langle \Delta r(n)^2 \rangle}{n}. \tag{8}$$

It is well known that this later quantity may be ill defined in a 2D system because of the possible existence of a long-time $(1/t)$ tail in the velocity autocorrelation function [49]. The quantity might be strongly sensitive to the size dependence. In our case we tested results by increasing the number of particles times two and times three and in each case the results were in agreement. The normal pseudodiffusion coefficient decreases monotonically with increasing density at constant temperature. For the MB model of water there is a region where the coefficient increases.

A structural anomaly was assessed by determining the translational order parameter t and two orientational order parameters (with three-fold symmetry q_3 and with six-fold symmetry q_6). The translational order parameter measures the degree of pair correlation in the system and is defined as

$$t = \int_0^{x_c} |g(x) - 1| dx, \tag{9}$$

where $x = \rho^{\frac{1}{2}} r$ is the distance r in the units of mean interparticle separation and $g(x)$ the pair distribution function.

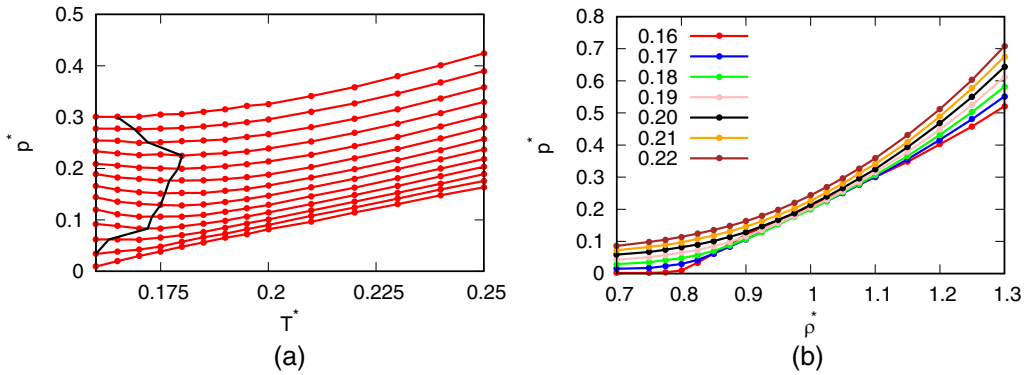

FIG. 4. (a) The pressure as a function of temperature for different densities. Red lines correspond to isochores from bottom up for densities 0.8, 0.825, 0.85, 0.875, 0.9, 0.925, 0.95, 0.975, 1.0, 1.025, 1.05, 1.075, 1.1. Black line connects points with maximum density for different temperatures. (b) Pressure as a function of density for different temperatures.

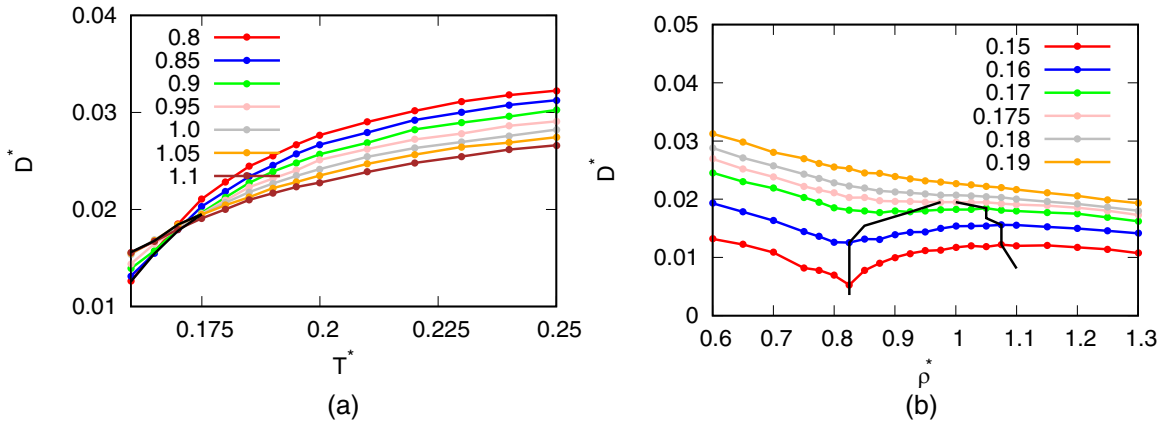

FIG. 5. (a) The pseudodiffusion coefficient as a function of the temperature for several isochores and (b) the density for several isotherms. Black lines connect points with maximum and minimum of the pseudodiffusion coefficient.

x_c is the cut off distance and is set to half of the simulation box in the present paper. For normal fluids the translational order parameter monotonically increases with density. If a different behavior is observed in a certain density range, the fluid is said to exhibit a structural anomaly. Orientational order parameters q_l were calculated following this procedure. For each particle j we calculate

$$q_l^j = \frac{1}{n_j} \sum_k \exp(il\theta_{jk}), \tag{10}$$

where n_j is the number of neighbors within the first atom shell of particle j and θ_{jk} is the angle between the vector connecting particles j and k and the horizontal axis. Parameter l specifies the type of symmetry (3 or 6). The local orientational parameter of the whole system is calculated as the average of the absolute value over all the particles in the system

$$q_l = \frac{1}{N} \sum_{i=1}^{N} |q_l^i|. \tag{11}$$

The excess entropy is a convenient quantity for understanding the links between structure and thermodynamics, as well as dynamics. To calculate the excess entropy we should count all the accessible configurations for a fluid and compare it to the ideal gas entropy. The excess entropy can also be calculated by the multiparticle correlation expansion

$$s_e = s_2 + s_3 + \cdots + s_n + \cdots, \tag{12}$$

where s_n denotes the entropy contribution due to n-particle correlations. The effect of triplet and higher-order correlations on the entropy has not been extensively studied, the pair entropy itself proves to be a very convenient structural estimator for the entropy. The pair entropy can be approximated by

$$s_2 = -\pi\rho \int [g(r)\ln g(r) - g(r) + 1] r dr, \tag{13}$$

and is the dominant contribution to excess entropy [50–60]. Integration was up to half the length of the simulation box. The pair entropy is proved to be between 85% and 95% of the total excess entropy in Lennard-Jones systems [51]. At higher temperatures we determined excess entropy by the Widom method and we observed similar agreement for the MB model as reported for LJ systems. The pair entropy only depends on the pair correlation function $g(r)$ and the density and it is related to the translations order parameter because both are related to the deviation of the radial distribution function from unity.

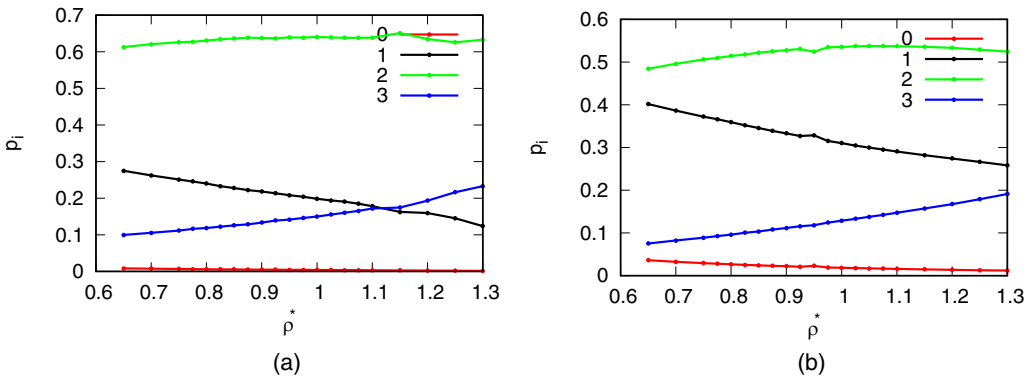

FIG. 6. Ratio of differently bonded water molecules for different isochores for (a) at temperature $T^* = 0.16$, (b) at $T^* = 0.20$.

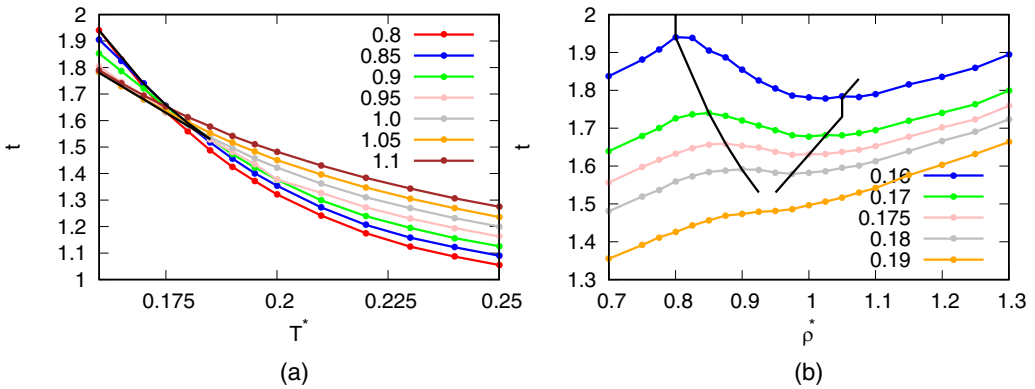

FIG. 7. (a) The translational order parameter as a function of the temperature for several isochores and (b) the density for several isotherms. Black lines connect points with maximum and minimum of the translational order parameter.

IV. RESULTS AND DISCUSSION

All our results were calculated and are reported in reduced units; the excess internal energy and temperature are normalized to the HB energy parameter $\varepsilon_{\mathrm{HB}}$ ($A^* = \frac{A}{|\varepsilon_{\mathrm{HB}}|}$, $T^* = \frac{k_B * T}{|\varepsilon_{\mathrm{HB}}|}$) and the distances are scaled to the hydrogen bond characteristic length r_{HB} ($r^* = \frac{r}{r_{\mathrm{HB}}}$). Errors in the MC simulations depend on temperature, for most of the temperatures are of size of the symbols used to present data points.

The 2D MB model of water has water-like behavior as reported before [28]. The density of low density ice (see Fig. 2) is lower than the density of the liquid phase. The two most important crystal phases of 2D MB water are low density crystal with reduced density 0.7698 where water molecules occupy positions in a hexagonal lattice. There is only one possible crystalline arrangement that permits the maximum number of perfect hydrogen bonds per molecule. This low-density crystal structure is analogous to hexagonal ice Ih, and it is also the crystalline phase that has been observed in low-temperature Monte Carlo simulations of the MB model [28]. The 2D MB water also has denser forms of ice at high pressures. One possible candidate for the high density crystal phase is where another water molecule occupy empty spaces in hexagons (see Fig. 2). This phase conforms to a triangular packing arrangement. The reduced density of the high density crystal phase is 1.1547. We should take into account that the two ices described above do not exhaust the possible crystalline structures for this model. When the MB water melts, the structure of low density ice is present a lot also in liquid water. Figure 3 shows the phase diagram of

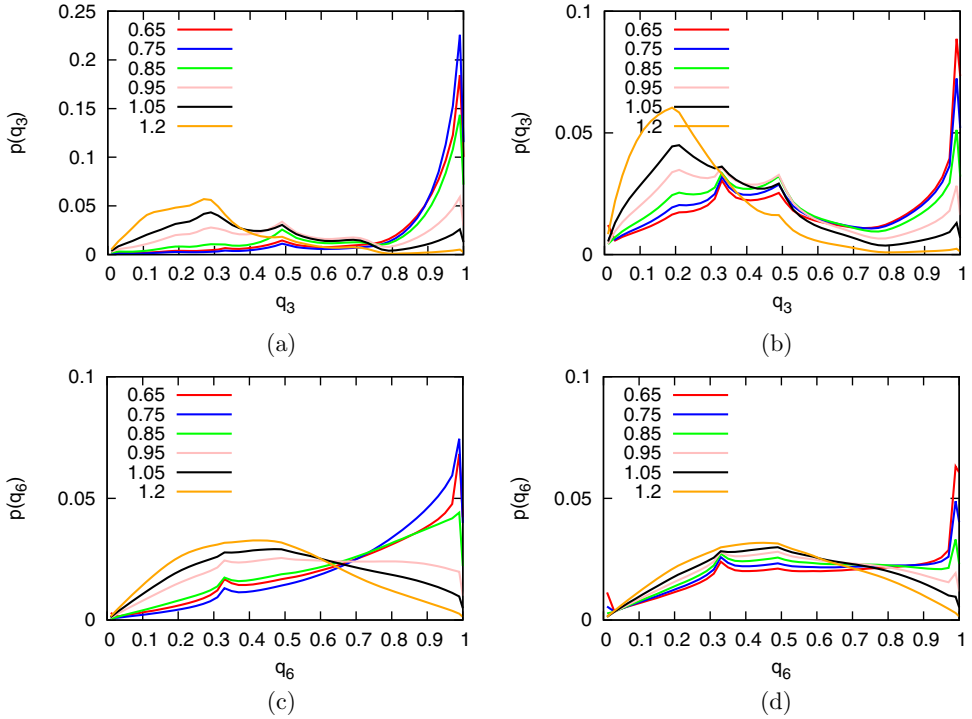

FIG. 8. The distribution of the different order parameters for different isochores for (a) three-fold parameter at temperature $T^* = 0.15$, (b) at $T^* = 0.20$, and for (c) six-fold parameter at temperature $T^* = 0.15$, (d) at $T^* = 0.20$.

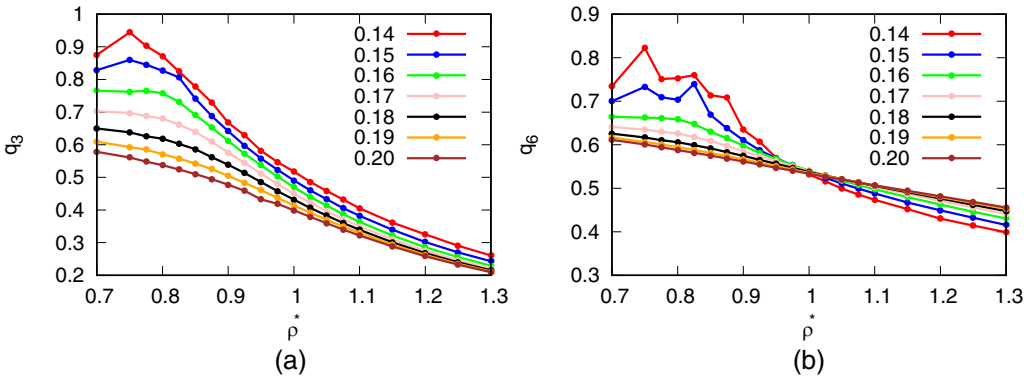

FIG. 9. (a) The orientational order parameter with three fold symmetry and (b) the orientational order parameter with six-fold symmetry against density for several isotherms.

the MB model since the freezing (melting) coexistence lines are relevant to locate if some thermodynamic points fall in the metastable regions of the model. As we can see from the phase diagram the anomalous regions are present in fluid part of phase diagram and extend also in supercooled region.

First we determine density anomaly. We can do this by calculating the density as a function of temperature at constant pressure and observe the density maximum at certain pressures. This was done for selected pressures before [28]. There is an alternative way to determine the temperature of maximum density. This is by calculating pressure as a function of density at constant temperature. Where the density maximum is present we observe a minimum in pressure as a function of density. Several isochores are presented in Fig. 4 as well as a line showing temperatures of maximum density. For the model we observe density anomaly for the temperatures lower that 0.18 and for the densities between 0.8 and 1.1 and for the pressures between 0.05 and 0.3. This is in a small region between the density of low and high crystal phases. The origin of the density anomaly is that at lower temperatures water still has a lot of low density ice structure present in the liquid phase. These structures are melting. Water molecules which are released from crystal structures occupy empty spaces between hexagons and the density of liquid increases. Upon further increase of temperature, hydrogen bonds continue to melt and more opened structures are formed which has lower density. At higher temperature such crystal water structures are no longer present and there is no density anomaly. Water behaves as a normal liquid where density decreases with the increase of temperature at a constant pressure.

We continued our calculation by determining the density anomaly. We calculated the pseudodiffusion coefficient by the displacement of water molecules in the MC steps at a fixed maximum step. This pseudodiffusion coefficient is proportional to real diffusion coefficient of the 2D MB model. For normal fluids the diffusivity decreases monotonically with increasing density at constant temperature because with the increase of density there is more crowding and molecules move with higher difficulty. For the 2D MB model this is observed only for temperatures higher than 0.175. For temperatures lower that 0.175 diffusion has anomalous behavior. At first the diffusion decreases, reaches minimum, increases up to maximum and decreases toward zero for high densities. The region between the minimum and the maximum is the so-called anomalous diffusion region and is presented in Fig. 5. This anomaly region is also present in the density range between the high and low density ices. As the density increases at constant temperature the water forms a more correct hexagonal network and a little after the density of low density crystal phase diffusion has hit minimum. Upon further increase of the density water molecules occupy empty space within the hexagons and diffusion start to increase since these molecules are less bonded than molecules forming HB networks and can move more easily. Upon further increase of

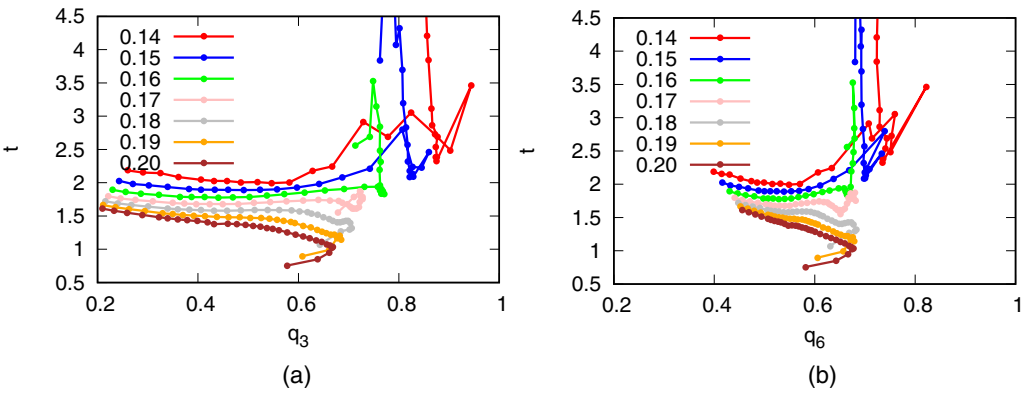

FIG. 10. (a) The $t - q_3$ order map and (b) the $t - q_6$ plane.

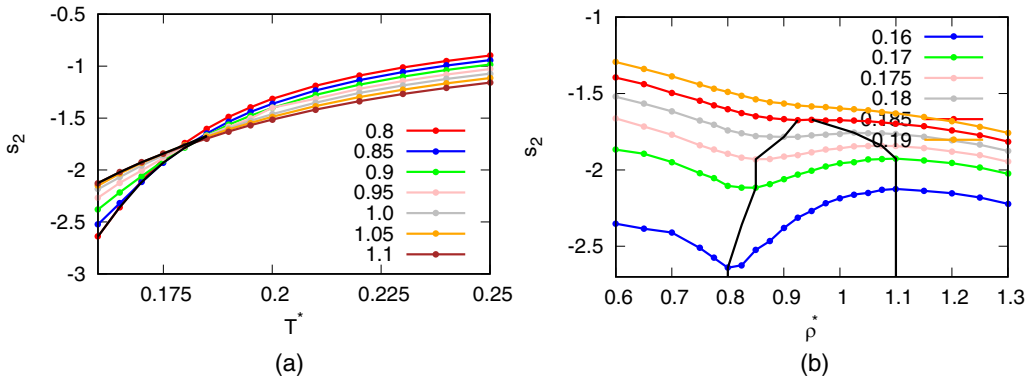

FIG. 11. (a) The pair entropy as a function of the temperature for several isochores and (b) the density for several isotherms. Black lines connects points with maximum and minimum of the pair entropy.

the density the system reaches such density that the mobility of molecules reaches maximum and upon further increase less and less space is available and the molecules move with bigger difficulty and diffusion starts to decrease. What is unexpected is that this diffusion anomalous region lies within the density anomalous region. In water-like models and in silica-like models the density anomalous region is the most inner region. The reason for this is not completely clear, one reason might be the dimensionality of the system. Here we have the 2D model with water-like properties or we can have the model that is not completely water- or silica-like but has its unique properties. Since the diffusion is related to the ability of water molecules to move we plotted in Fig. 6 the ratio of differently bonded water molecules. We would expect that when the diffusion of water is smaller that water molecules would be strongly bonded, or on the other hand, would not have available space to move. We would expect some unusual behavior, but on the contrary these properties do not have anything unusual. All functions are monotonic functions with respect to temperature so they do not give us any new insight for the diffusion anomaly with respect to strong bonding.

Thirdly, we studied the structural behavior by calculating three different quantities, the translational order parameter t and two orientational order parameters, q_3 orientational order with three-fold axis and q_6 orientational order with six-fold axis. For the normal fluids, t increases with increasing density. For the 2D MB model we found this monotonic behavior only for the temperatures higher that 0.19 (see Fig. 7). For lower temperatures we observe that the t has a maximum, decreases up to a minimum, and recovers the normal increasing behavior after the minimum. The region between the minimum and maximum is called the anomalous structure region. Figure 8 shows the distribution of both orientational order parameters for low and high temperatures for different densities. We can see that at the densities close to the density of the low density ice we can see a huge peak for three-fold symmetry. Upon the increase of density we can see that other structures start to appear. We can observe additional peaks in distribution. Our study reveals the anomalous behavior also for both orientational order parameters. For the temperatures higher than 0.16 both parameters decrease with the increase of density. For temperatures lower that 0.16 we can observe a maximum close to the density of low density ice phase. This is presented in Fig. 9.

The order map in the $t - q_3$ and $t - q_6$ plane plotted in Fig. 10 resembles the one observed for water and other two-scale potentials reported before [10–13]. There are two different regimes present for both plots. For the temperatures belonging to the structural anomalous region we can observe curves to form closed loops while for higher temperatures curves turn in the opposite direction without forming closed loops for both orientational parameters.

The region of entropy anomaly is given by the condition that the entropy of the liquid increases on compression. Maxwell's relation relates the condition for entropy anomaly to the isothermal compressibility and the sign of the thermal

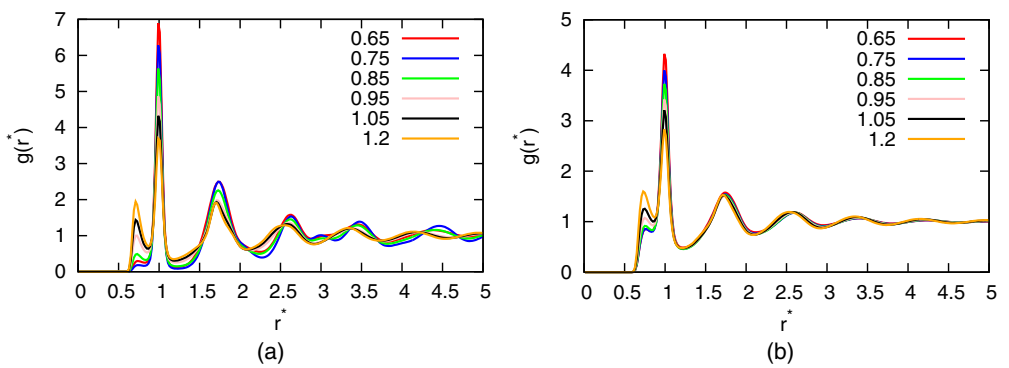

FIG. 12. The pair correlation functions for different isochores for (a) at temperature $T^* = 0.15$, (b) at $T^* = 0.20$.

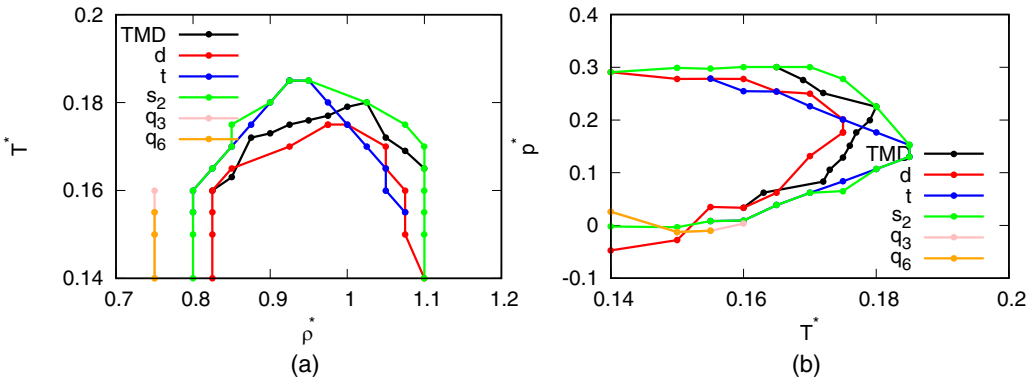

FIG. 13. (a) The temperature-density plane containing all the anomalies found for the 2D MB model of water. Colors of lines are explained by legend. (b) Same as in (a) but for pressure temperature plane.

expansion coefficient

$$\left(\frac{\partial s}{\partial \rho}\right)_T = -V^2 \frac{\alpha}{\kappa_T}. \tag{14}$$

The relation shows that the entropy displays anomalous behavior in the region where the thermal expansion coefficient is negative. Since for a classical fluid $s = s_{\mathrm{id}} + s_e$, where s_{id} is the ideal gas entropy that has a monotonic dependence on the density, the condition for excess entropy anomaly corresponds to $(\partial s_e/\partial \rho)_T > 0$. The multiparticle correlation approximation expands the excess entropy as $s_e = s_2 + s_3 + + s_n$, so it may be expected that if the pair correlations dominate the entropy of the liquid, the pair entropy would provide an equivalent condition for finding the region of the entropy anomaly and this is what we did. In Fig. 11 we plotted pair entropy as a function of density and temperature and we observed an anomalous region. In Fig. 12 we plotted pair correlation functions for two different temperatures for several densities to try and see what might be the reason for anomalies. We can see that at low temperature there is long-range structure change and we believe this is the reason for anomalies, but it does not give us insight on the hierarchy of them.

In Fig. 13 we plotted the relation between the several anomalies presented for the 2D MB model of water. The errors of the quantities are the size of the symbols. The temperature of the maximum density line lies between the diffusion and entropy anomaly. There is a difference between the positions of the structure and entropy anomaly. The hierarchy of anomalies found here is different than the one reported for the SPC/E water, other two-scale potentials [10–13,61] and a double-Gaussian fluid [62]. Prestipino *et al.* [63] showed that the anomalous thermodynamic behavior may occur also for weakly softened potentials, i.e., simple fluids characterized by a repulsion that is only marginally softened and yields a single structure at a local level. The most inner is the diffusion anomaly, then density, and then structural. In a water-like hierarchy we have density, diffusion, and structural while in a silica-like hierarchy we have density, structural, and diffusion. Why the 2D MB model has a different hierarchy might be related to dimensionality or a combination of different effects. For the coarse-grained model of a water monolayer between hydrophobic walls at partial hydration, the density anomaly is included in the diffusion anomaly region, as in water [64]. For an associating lattice gas (ALG) model which combines a two-dimensional lattice gas with particles interacting through a soft core potential and orientational degrees of freedom [65], the diffusion anomaly is included in the density anomaly region, as in the present model. A similar hierarchy has been found also for models in three dimensions [66] although never observing also the structural anomaly.

V. CONCLUSION

The Monte Carlo simulations were used to predict the hierarchy of anomalies in the 2D MB model of water. The MB model balances the Lennard-Jones interactions with an orientation dependence that is intended to mimic hydrogen bonding. The MB model has previously been shown to have the volume anomalies of pure water and the thermal anomalies of nonpolar solvation. Beside the known density anomaly it was discovered that the MB model also has structure and diffusion anomalies. The diffusion anomaly has the smaller region and is encompassed by the density anomalous region and this one by the structure anomalous region. This is slightly different as in the real water where the anomalies are in order of density, diffusion, and structure or in the silica-like models where the anomalies are in order of density, structure, and diffusion.

ACKNOWLEDGMENTS

This work was supported by the NIH (GM063592) and Slovenian Research Agency (P1 0103-0201, N1-0042) and the National Research, Development, and Innovation Office of Hungary (SNN 116198).

[1] R. Sharma, S. N. Chakraborty, and C. Chakravarty, J. Chem. Phys. **125**, 204501 (2006).

[2] M. S. Shell, P. G. Debenedetti, and A. Z. Panagiotopoulos, Phys. Rev. E **66**, 056703 (2002).

[3] P. H. Poole, M. Hemmati, and C. A. Angell, Phys. Rev. Lett. **79**, 2281 (1997).
[4] J. M. Kincaid and G. Stell, Phys. Lett. A **65**, 131 (1978).
[5] P. Lamparter, S. Stieb, and W. Knoll, Z. Naturforsch. A **31**, 90 (1976).
[6] H. Thurn and J. Ruska, J. Non-Cryst. Solids **22**, 331 (1976).
[7] G. E. Sauer and L. B. Borst, Science **158**, 1567 (1967).
[8] C. A. Angell, E. D. Finch, and P. Bach, J. Chem. Phys. **65**, 3063 (1976).
[9] F. X. Prielmeier, E. W. Lang, R. J. Speedy, and H.-D. Ludemann, Phys. Rev. Lett. **59**, 1128 (1987).
[10] J. R. Errington and P. G. Debenedetti, Nature (London) **409**, 318 (2001).
[11] P. A. Netz, F. W. Starr, H. E. Stanley, and M. C. Barbosa, J. Chem. Phys. **115**, 344 (2001).
[12] A. B. de Oliveira, G. Franzese, P. A. Netz, and M. C. Barbosa, J. Chem. Phys. **128**, 064901 (2008).
[13] G. Franzese, G. Malescio, A. Skibinsky, S. V. Buldyrev, and H. E. Stanley, Nature (London) **409**, 692 (2001).
[14] W. L. Jorgensen, J. Chandrasekhar, J. D. Madura, R. W. Impey, and M. L. Klein, J. Chem. Phys. **79**, 926 (1983).
[15] I. Nezbeda, J. Mol. Liq. **73-74**, 317 (1997).
[16] B. Guillot, J. Mol. Liq. **101**, 219 (2002).
[17] C. Vega, J. L. F. Abascal, M. M. Conde, and J. L. Aragones, Faraday Discuss. **141**, 251 (2009).
[18] T. M. Truskett, P. G. Debenedetti, S. Sastry, and S. Torquato, J. Chem. Phys. **111**, 2647 (1999).
[19] K. A. Dill, T. M. Truskett, V. Vlachy, and B. Hribar-Lee, Annu. Rev. Biophys. Biomol. Struct. **34**, 173 (2005).
[20] I. Nezbeda, J. Kolafa, and Yu. V. Kalyuzhnyi, Mol. Phys. **68**, 143 (1989).
[21] I. Nezbeda and G. A. Iglezias-Silva, Mol. Phys. **69**, 767 (1990).
[22] A. L. Balladares, V. B. Henriques, and M. C. Barbosa, J. Phys.: Condens. Matter **19**, 116105 (2007).
[23] M. Girardi, M. Szortyka, and M. C. Barbosa, Physica A (Amsterdam) **386**, 692 (2007).
[24] M. M. Szortyka, C. E. Fiore, V. B. Henriques, and M. C. Barbosa, J. Chem. Phys. **133**, 104904 (2010).
[25] G. Franzese and H. E. Stanley, J. Phys.: Condens. Matter **14**, 2201 (2002).
[26] V. Bianco and G. Franzese, Sci. Rep. **4**, 4440 (2014).
[27] G. Andaloro and R. M. Sperandeo-Mineo, Eur. J. Phys. **11**, 275 (1990).
[28] K. A. T. Silverstein, A. D. J. Haymet, and K. A. Dill, J. Am. Chem. Soc. **120**, 3166 (1998).
[29] K. A. T. Silverstein, K. A. Dill, and A. D. J. Haymet, Fluid Phase Equilib. **150-151**, 83 (1998).
[30] N. T. Southall and K. A. Dill, J. Phys. Chem. B **104**, 1326 (2000).
[31] K. A. T. Silverstein, A. D. J. Haymet, and K. A. Dill, J. Chem. Phys. **114**, 6303 (2001).
[32] A. Ben-Naim, J. Chem. Phys. **54**, 3682 (1971).
[33] A. Ben-Naim, Mol. Phys. **24**, 705 (1972).
[34] C. L. Dias, T. Hynninen, T. Ala-Nissila, A. S. Foster, and M. Karttunen, J. Chem. Phys. **134**, 065106 (2011).
[35] C. L. Dias, Phys. Rev. Lett. **109**, 048104 (2012).
[36] A. Bizjak, T. Urbic, V. Vlachy, and K. A. Dill, Acta Chim. Slov. **54**, 532 (2007).
[37] A. Bizjak, T. Urbic, V. Vlachy, and K. A. Dill, J. Chem. Phys. **131**, 194504 (2009).
[38] C. L. Dias, T. Ala-Nissila, M. Grant, and M. Karttunen, J. Chem. Phys. **131**, 054505 (2009).
[39] T. Urbic, V. Vlachy, Yu. V. Kalyuzhnyi, N. T. Southall, and K. A. Dill, J. Chem. Phys. **112**, 2843 (2000).
[40] T. Urbic, V. Vlachy, Yu. V. Kalyuzhnyi, N. T. Southall, and K. A. Dill, J. Chem. Phys. **116**, 723 (2002).
[41] T. Urbic, V. Vlachy, Yu. V. Kalyuzhnyi, and K. A. Dill, J. Chem. Phys. **118**, 5516 (2003).
[42] T. Urbic, V. Vlachy, O. Pizio, and K. A. Dill, J. Mol. Liq. **112**, 71 (2004).
[43] T. Urbic, V. Vlachy, Yu. V. Kalyuzhnyi, and K. A. Dill, J. Chem. Phys. **127**, 174511 (2007).
[44] T. Urbic and M. F. Holovko, J. Chem. Phys. **135**, 134706 (2011).
[45] T. Urbic, Phys. Rev. E **96**, 032122 (2017).
[46] J. P. Hansen and I. R. McDonald, *Theory of Simple Liquids* (Academic, London, 1986).
[47] D. Frenkel and B. Smit, *Molecular Simulation: From Algorithms to Applications* (Academic, New York, 2000).
[48] S. Prestipino, F. Saija, and P. V. Giaquinta, J. Chem. Phys. **137**, 104503 (2012).
[49] P. J. Camp, Phys. Rev. E **71**, 031507 (2005).
[50] H. J. Raveche, J. Chem. Phys. **55**, 2242 (1971).
[51] A. Baranyai and D. J. Evans, Phys. Rev. A **40**, 3817 (1989).
[52] H. S. Green, *The Molecular Theory of Fluids* (North-Holland, Amsterdam, 1952).
[53] Y. Rosenfeld, J. Phys.: Condens. Matter **11**, 5415 (1999).
[54] J. Mittal, J. Chem. Phys. **125**, 076102 (2006).
[55] J. Mittal, J. R. Errington, and T. M. Truskett, J. Phys. Chem. B **110**, 18147 (2006).
[56] S. N. Chakraborty and C. Chakravarty, Phys. Rev. E **76**, 011201 (2007).
[57] A. Scala, F. W. Starr, E. La Nave, F. Sciortino, and H. E. Stanley, Nature **406**, 166 (2000).
[58] M. Agarwal, R. Sharma, and C. Chakravartya, J. Chem. Phys. **127**, 164502 (2007).
[59] M. Agarwal and C. Chakravarty, J. Phys. Chem. B **111**, 13294 (2007).
[60] P. Vilaseca and G. Franzese, J. Chem. Phys. **133**, 084507 (2010).
[61] P. Vilaseca and G. Franzese, J. Non-Cryst. Solids **357**, 419 (2011).
[62] S. Prestipino, C. Speranza, G. Malescio, and P. V. Giaquinta, J. Chem. Phys. **140**, 084906 (2014).
[63] S. Prestipino, F. Saija, and G. Malescio, J. Chem. Phys. **133**, 144504 (2010).
[64] F. de los Santos and G. Franzese, J. Phys. Chem. B **115**, 14311 (2011).
[65] M. M. Szortyka and M. C. Barbosa, Physica A (Amsterdam) **380**, 27 (2007).
[66] P. A. Netz, S. V. Buldyrev, M. C. Barbosa, and H. E. Stanley, Phys. Rev. E **73**, 061504 (2006).